Supporting Information

From Phosphine-Stabilised towards Naked Au_8 Clusters through ZIF-8 Encapsulation

Table of Content

1. General Information

All chemicals were purchased from commercial suppliers and used without purification. All solvents were distilled prior to use. *Schlenk* technique and the glove box were used for carrying out the reactions under argon atmosphere. If necessary, the solvents were dried *via* the *MBraun MB SPS* purification system, additionally degassed using three freeze-pump-thaw cycles and stored over molecular sieves (3 or 4 Å). Deuterated solvents were purchased from *Eurisotop* and used without further purification.

^{1}H(400 MHz) and ^{31}P(162 MHz)-NMR were measured on *Bruker AVIII-400 US* or *Bruker DRX-400* spectrometers at 300 K/20 K. The NMR shift is specified relative to TMS and 85% H_3PO_4. The measured NMR-spectra were processed using MestReNova© (Version: 14.0.1-23559).

Samples were measured with a High-Resolution Transmission Electron Microscope Titan G2 (*FEI*) with Image corrector on accelerating voltage 80 kV. Images were taken with a BM UltraScan CCD camera (*Gatan*). STEM images were taken with HAADF detector 3000 (*Fishione*). Energy Dispersive Spectrometry (EDS) was performed in Scanning TEM (STEM) mode by Super-X system with four silicon drift detectors (*Bruker*).

Powder X-ray diffraction measurements were performed on a *PANalytical Empyrean* diffractometer equipped with a *PANalytical PIXcel* 1D detector. X-ray Cu K_α radiation (λ_1=1.5406 Å, λ_2=1.5444 Å, λ_1/λ_2=0.5) was used for the measurements, while K_β radiation was removed with a nickel filter. The voltage was 45 kV and the intensity 40 mA. The measurement range was from 5.08 to 50.08 (2θ) with a step size of 0.0408 (2θ) and an acquisition time of 35 seconds per step. Part of the measurements were carried out utilizing a *PANalytical Aeris* Benchtop PXRD under similar conditions.

The UV/Vis spectra were measured on a Cary 60 UV/Vis spectrometer from *Agilent Technologies*. All spectra were measured at room temperature in water as the solvent. Measurements were taken in the range 200-800 nm. The utilized cuvette was made out of SUPRASIL® quartz glass with a layer thickness of 10 mm.

The solid-state UV/Vis spectra were measured on a UV-3600 Plus with integrating sphere unit of the company *Shimadzu*. The reflection of the sample was measured in the range 200-800 nm. For the recording of the UV/Vis spectra, the samples were put between two microscope slides. As a reference barium sulphate was used.

Adsorption measurements with N_2 at 77 K were carried out on a 3Flex Physisorption from *Micromeritics Instrument Corp.* Adsorption data was processed using the 3Flex Software Version 5.01 by *Micromeritics Instrument Corp.* and plotted in OriginPro 2019b by *OriginLab Corp.* Samples were transferred into preweighed sample tubes and capped with Micromeritics CheckSeals. Samples were subsequently activated again at room temperature for 12 h under dynamic vacuum of ~ 10^{-3} mbar using a SmartVac Prep by *Micromeritics Instrument Corp.* to ensure absence of unwanted adsorbates and identical pre-measurement states of all samples. The mass of the adsorbent was then recorded, generally in the range of 25 - 100 mg. A liquid nitrogen bath is used for the measurements at 77 K. The surface area of the materials was derived using the Brunauer-Emmett-Teller model, is hence given as the 'BET surface' and based on N_2-isotherms measured at 77 K. The apparent surface area of the materials was derived using the BET model, is hence given as the 'BET area' and based on N_2 isotherms measured at 77 K. For microporous materials, to determine the apparent BET area – or the more precise BET capacity – care was taken to adhere to the Rouquerol criteria.[1,2]

A TGA/STA 409 PC apparatus from Mettler-Toledo Intl. Inc. was used for thermogravimetric analysis under synthetic air as specified with a continuous heating ramp of 10 °C/min. The corresponding evaluation software was STARe 14.00. For mass spectrometry a Thermostar GSD 320 T from Pfeiffer Vacuum GmbH was connected to the setup enabling a correlation between mass change, the fragment responsible, and the temperature. Roughly 5 mg of sample were applied per measurement.

For the MAS-NMR measurements the *Bruker Avance 300* was used with a frequency of 300 MHz for ^{1}H-, 75 MHz for ^{13}C- and 121 MHz for ^{31}P-NMR spectroscopy. All measurements were carried out at r.t. in a 4 mm ZrO_2 rotor fixed to a 4 mm MAS-probe head at a rotation frequency of 15 kHz (or 8 kHz). The ^{1}H-spectra were recorded with "single pulse technique", the ^{13}C-spectra with "cross polarisation" (CPMAS) and the ^{31}P-spectra with “high power decoupling” (HPDEC). The external standard for ^{1}H- and ^{13}C-measurements was adamantane with a chemical shift of 2.00 ppm and 29.47 ppm (both vs. TMS), respectively. $NH_4H_2PO_4$ with a chemical shift of 1.11 ppm was utilized as the external standard for the ^{31}P-NMR-measurements (vs. $H_3PO_{4\,\text{conc.}}$, with 0.00 ppm).

X-ray photoelectron spectra were recorded on a *Leybold-Heraeus* LHS 10 spectrometer using a non-monochromatized Al K_α source (1486.7 eV). The powder samples were pressed into cavities and measured as pellets. All spectra were acquired in an ultra-high vacuum chamber at a pressure below 5×10^{-8} mbar. The analyzer was operated at a constant pass energy of 100 eV leading to an energy resolution with a full width at half-maximum (FWHM) of ~1.1 eV. The energy scale of the spectra was corrected for sample charging by using the C 1s main signal (284.8 eV, adapted from literature for ZIF-8).[3,4] The intensity of all spectra was scaled to the total peak area of Zn $2p_{3/2}$. Core level spectra were deconvoluted by using Voigt functions and linear background subtraction.

The Elemental Analyzer (*Euro EA*) was used to quantify C, H, N, S *via* flash combustion and subsequent chromatographic separation. Zn and Au were analyzed by AAS (Atomic Absorption Spectroscopy) utilizing an *Agilent Technologies 200* (280FS AA). The quantification of Ti and P was carried out photometrically applying *Agilent Technologies Cary Serie UV-Vis Spectrophotometer* (Cary 100 UV-Vis).

2. Synthesis Protocol

$[Au_8(TPPMS)_x](NO_3)_2$ (x = 7,8)[5]

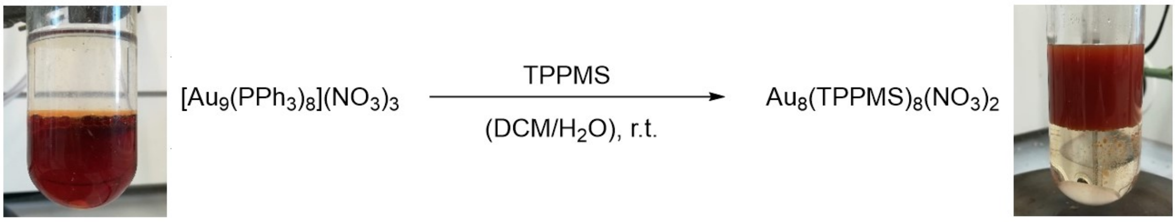

40.8 mg of TPPMS (112 µmol, 9.11 eq.) were dissolved in 30 mL of degassed H_2O and added to a solution of 49.7 mg of $[Au_9(PPh_3)_8](NO_3)_3$ (12.3 µmol, 1.00 eq.) in 30 mL of degassed dichloromethane under argon atmosphere. The two-layer reaction mixture was stirred for 1 h at r.t., the layers were separated, and the aqueous layer was centrifuged. The supernatant was dried *in vacuo* and 28.0 mg (6.59 µmol, *55%*) of a brown shiny solid was received.

^{31}P-NMR (162 MHz, D_2O, 300 K): δ 54.4 ppm.

^{1}H-NMR (400 MHz, D_2O, 300 K): δ 7.51 (m, 1H), 7.20 (m, 4H), 7.09 (m, 4H), 6.76 (m, 4H), 6.39 (m, 1H).

UV/Vis (H_2O) : λ_{max} [nm] = 470, 415, 300.

Au_8@ZIF-8 samples

A solution of 24.0 mg of $[Au_8(TPPMS)_X](NO_3)_2$ (5.40 µmol, 0.0048 eq.) in 2.5 mL of H_2O and 5.78 g of 2-methylimidazole (70.4 mmol, 70.4 eq.) dissolved in 20 mL of H_2O were added subsequently to a solution of 298 mg of $Zn(NO_3){\cdot}6H_2O$ (1.00 mmol, 1.00 eq.) in 2 mL of H_2O. This suspension was stirred for 5 min, centrifuged, washed with H_2O (2 × 7.5 mL) and dried *in vacuo*. 240 mg of the raw product was obtained and heated up to 200 °C under vacuum for 2 h to get rid of the guest molecules trapped in the pores yielding 200 mg (0.77 mmol, *77%)* of **Au_8@ZIF-8** as a brown powder.

AAS Au loading: ~3.3%

UV/Vis-DR: λ_{max} [nm] = 415, 470.

^{31}P-MAS-NMR (121 MHz, 297.15 K): δ 57.8, 32.0, −4.3 ppm.

BET surface area (N_2, 77 K) [m^2/g]: 1530.

For low gold loading samples, 6.8 mg of $[Au_8(TPPMS)_X](NO_3)_2$ (1.47 µmol, 0.0010 eq.) was used affording 196 mg of the raw product and ultimately yielding 170 mg of a pale yellow powder (0.74 mmol, *74%).*

AAS Au loading: ~1.1%

For high gold loading samples, 66.0 mg of $[Au_8(TPPMS)_X](NO_3)_2$ (14.30 µmol, 0.014 eq.) was used affording 276 mg of the raw product and ultimately yielding 212 mg of a dark brown powder (0.72 mmol, *72%).*

AAS Au loading: ~8.2%

Oxygen Treatment

For the oxygen treatment, Au_8@ZIF-8 materials were transferred into a *Fisher-Porter* tube that was put under vaccum and refilled with pure oxygen (purity 5.0, 1/3 bar_g) and subsenquently heated utilizing a sand bath to 150/200 °C for 2 h.

Heat Treatment

Au_8@ZIF-8 materials were transferred into a *Schlenk* tube or a ceramic crucible and then heated utilizing a tube furnace (for dynamic vacuum) or a muffle oven (for atmosphere-controlled experiments), respectively.

Vacuum Experiments: Samples were placed in a tube furnace preheated at the chosen temperature (T = 200, 250, 300 or 350 °C) for 1 h and allowed to cool down to room temperature. The same procedure was sequentially employed once (T = 250 °C), twice (T = 250 and 300 °C) and thrice (T = 250, 300 and 350 °C) to produce the corresponding 250, 300 and 350 °C samples. Characterisations of the temperature-treated samples were performed at room temperature after the corresponding heating step.

Atmosphere-Controlled Experiments Samples were heated from room temperature to the chosen temperature (T = 250, 300, 350 or 400 °C) with a heating rate of 5 K/min, held at that temperature for 1 h and allowed to cool down to room temperature. The same procedure was sequentially employed once (T = 300 °C), twice (T = 300 and 350 °C) and thrice (T = 300, 350 and 400 350 °C) to produce the corresponding 300, 350 and 400 °C samples. Characterisations of the temperature-treated samples were performed at room temperature after the corresponding heating step.

3. Characterisation

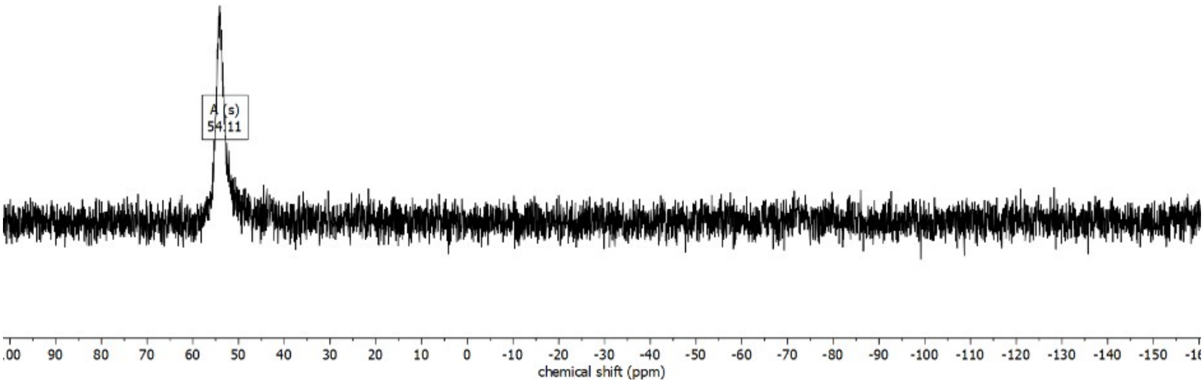

Figure S1: ^{31}P-NMR spectrum of the TPPMS-stabilised **Au$_8$** cluster in D_2O.

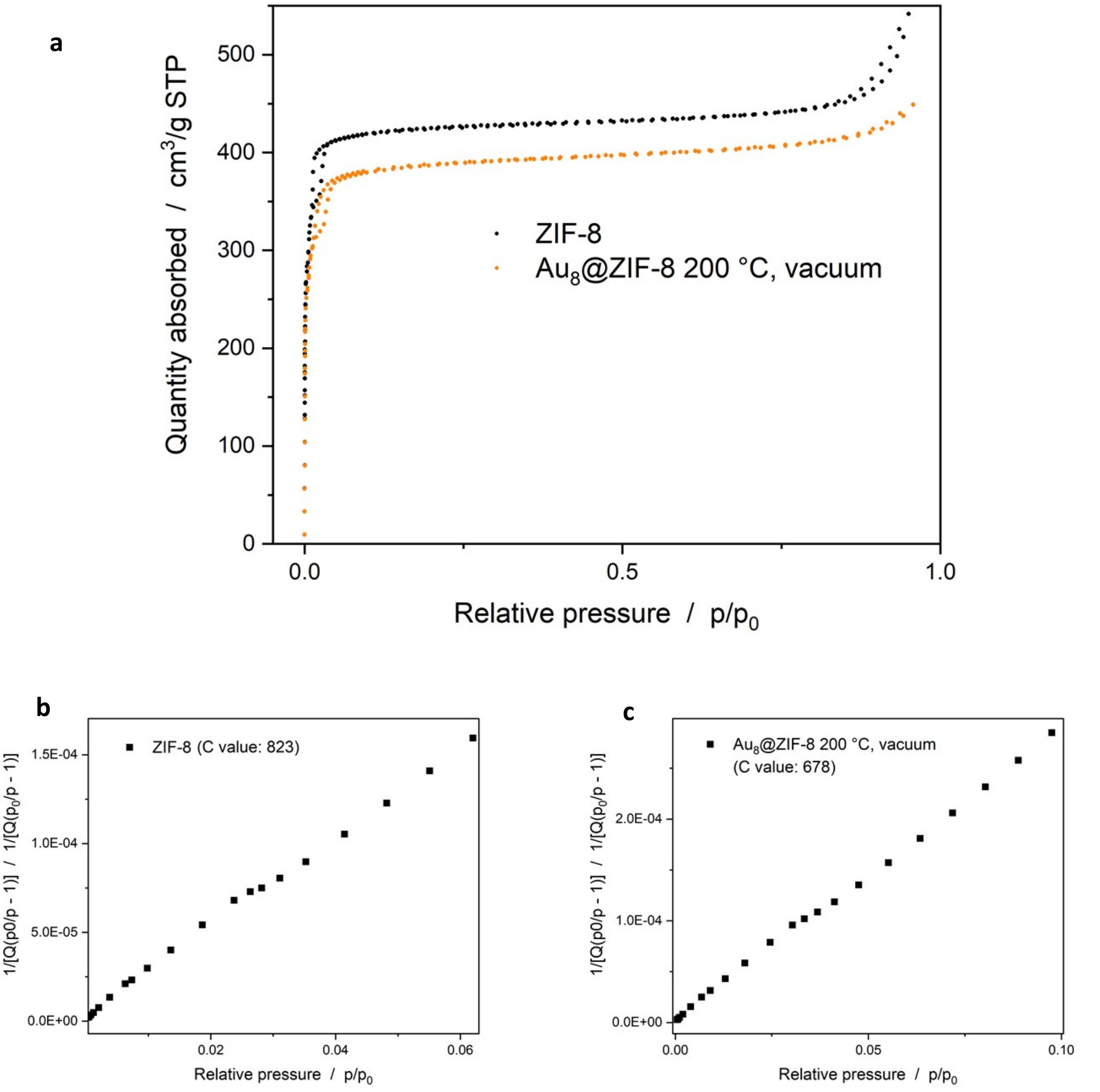

Figure S2: **a** N_2 BET isotherm of ZIF-8 and **Au$_8$@ZIF-8** after heating under dynamic vacuum at 200 °C, **b** and **c** respective BET surface area plots and C values.

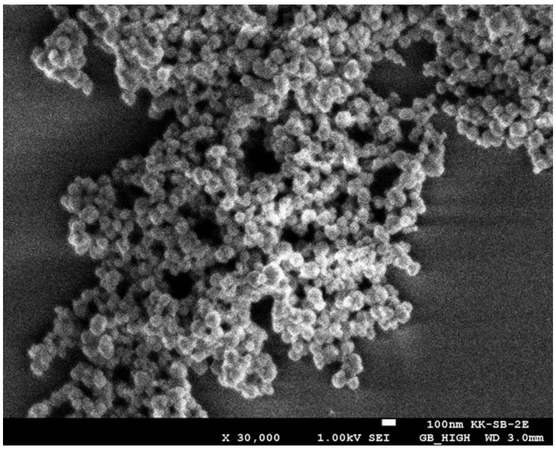

Figure S3: SEM image of **Au$_8$@ZIF-8**.

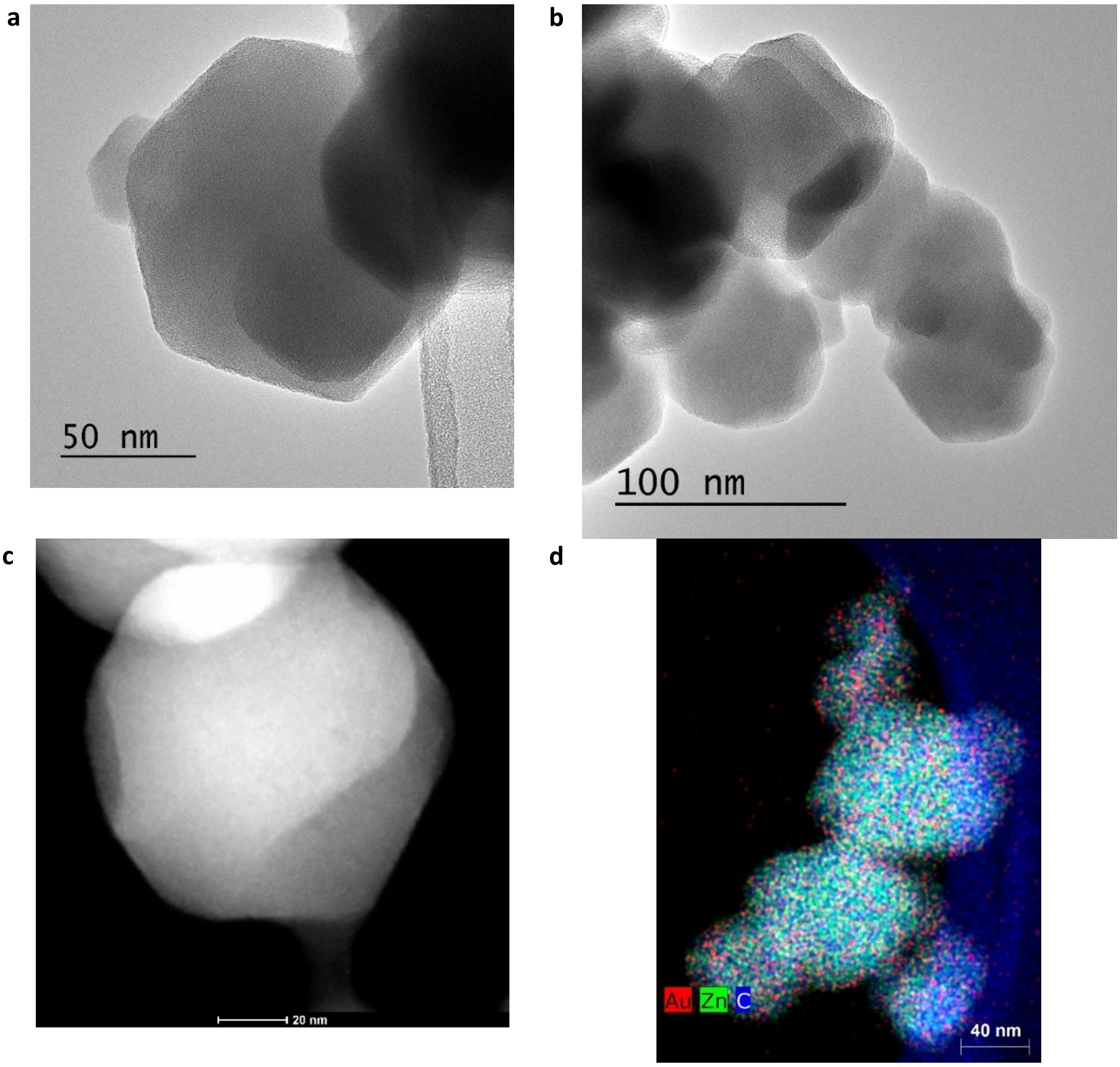

Figure S4: **a**, **b** HRTEM and **c** HAADF STEM of **Au$_8$@ZIF-8** and **d** elemental mapping.

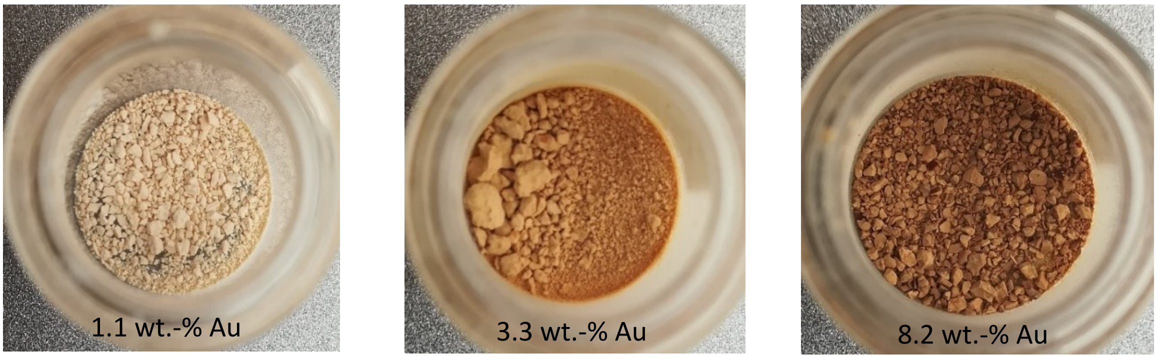

Figure S5: Pictures revealing the loading dependent colour of Au_8@ZIF-8 materials.

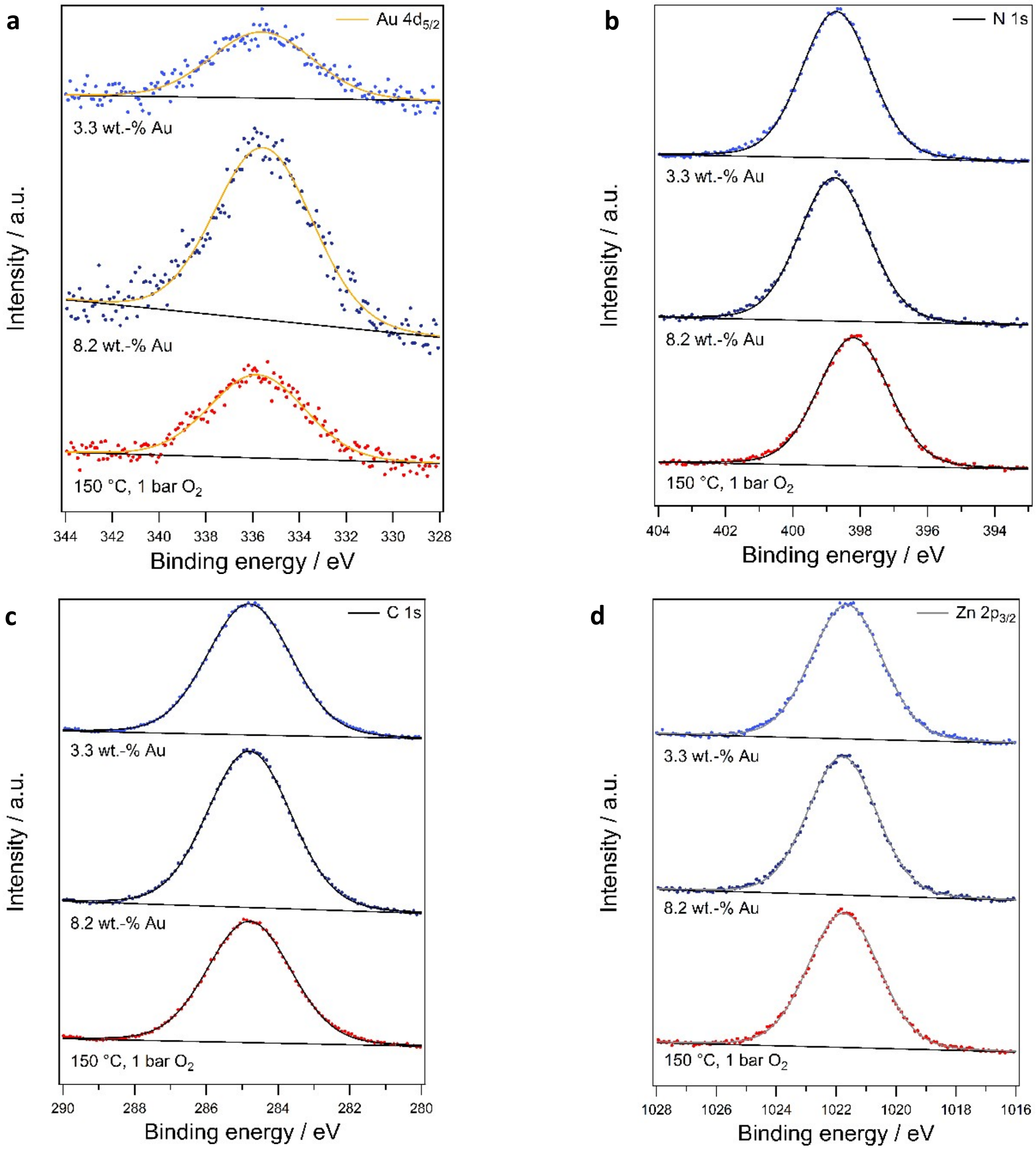

Figure S6: XPS spectra of the **a** Au $4d_{5/2}$, **b** N 1s, **c** C 1s and **d** Zn $2p_{3/2}$ region of Au_8@ZIF-8 materials with 3.3 and 8.2 wt.-% Au loadings and on **Au_8@ZIF-8** (3.3 wt.-% Au loading) after heating to 150 °C under 1 bar oxygen (red traces).

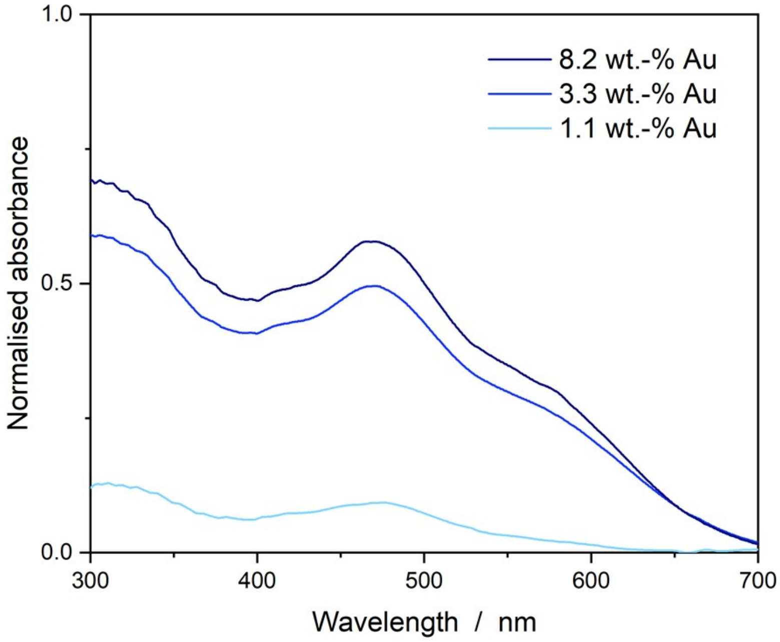

Figure S7: DR-UV/Vis spectra of Au_8@ZIF-8 materials with loading variations.

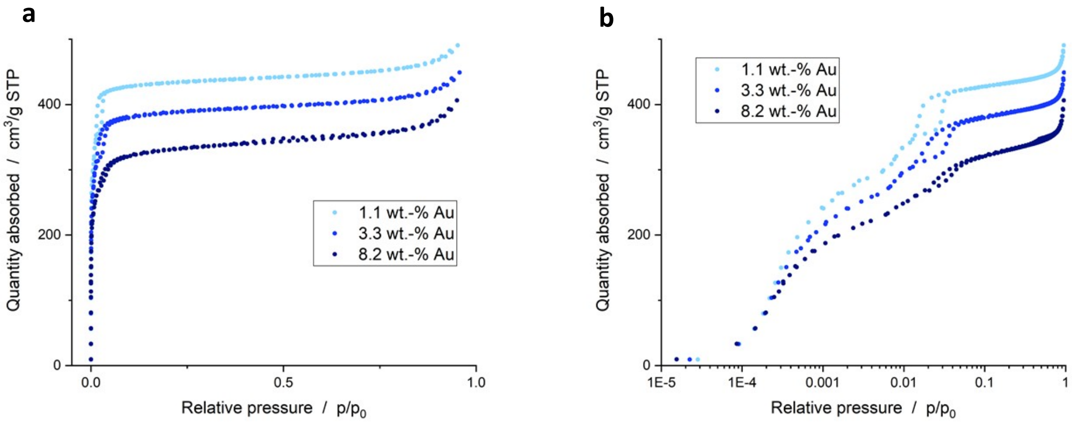

Figure S8: BET isotherms of Au_8@ZIF-8 materials with different Au loadings (**a**) and their semi-log plot (**b**).

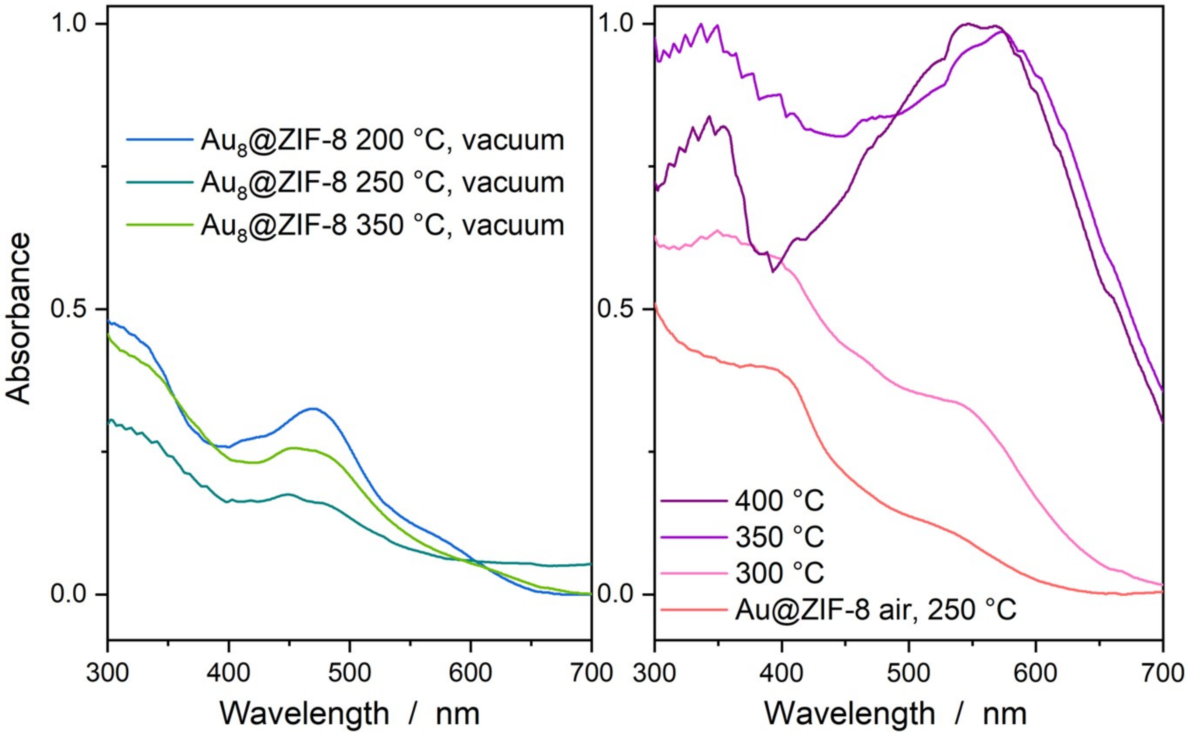

Figure S9: **a** UV/Vis-DR spectra of **Au$_8$@ZIF-8** heated at 200, 250 and 350 °C *in vacuo* and **b Au$_8$@ZIF-8** heated at 250, 300, 350 and 400 °C in air revealing cluster decomposition and AuNP formation (plasmonic resonance).

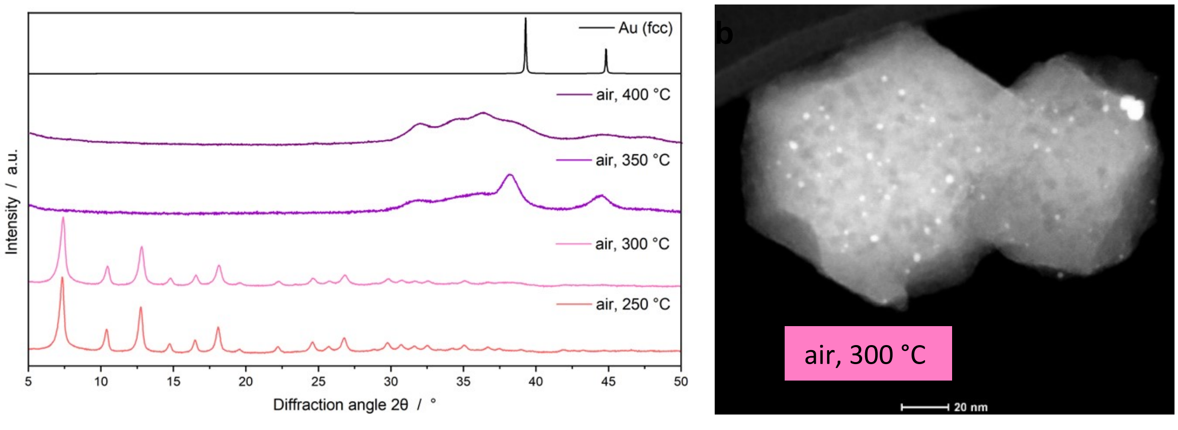

Figure S10: **a** PXRD of **Au$_8$@ZIF-8** after heat treatment under air at the respective temperatures in comparison with the pattern of Au (fcc) and **b** HAADF STEM of **Au$_8$@ZIF-8** sample after heat treatment at 300 °C under air revealing AuNP formation.[6]

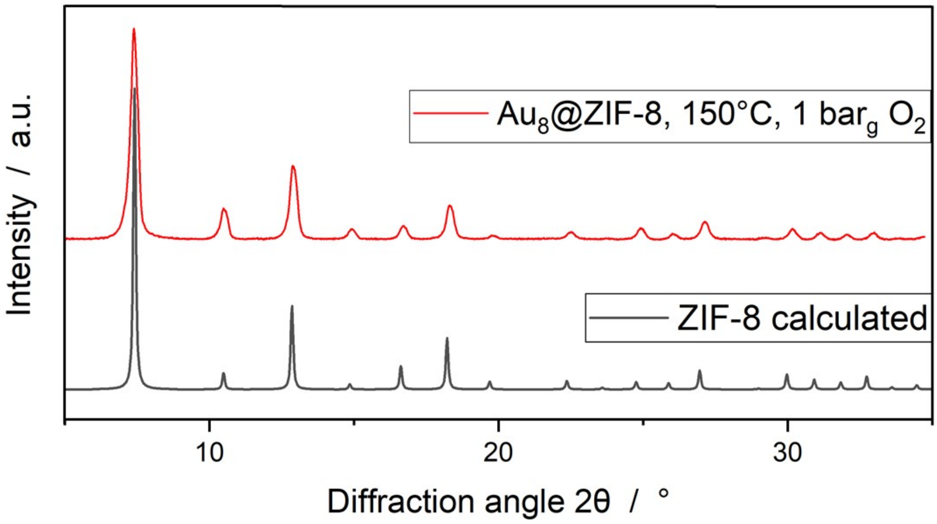

Figure S11: PXRD pattern of **Au$_8$@ZIF-8** after oxidative treatment (150 °C, 1 bar$_g$ O$_2$) and the calculated diffractogram of ZIF-8.

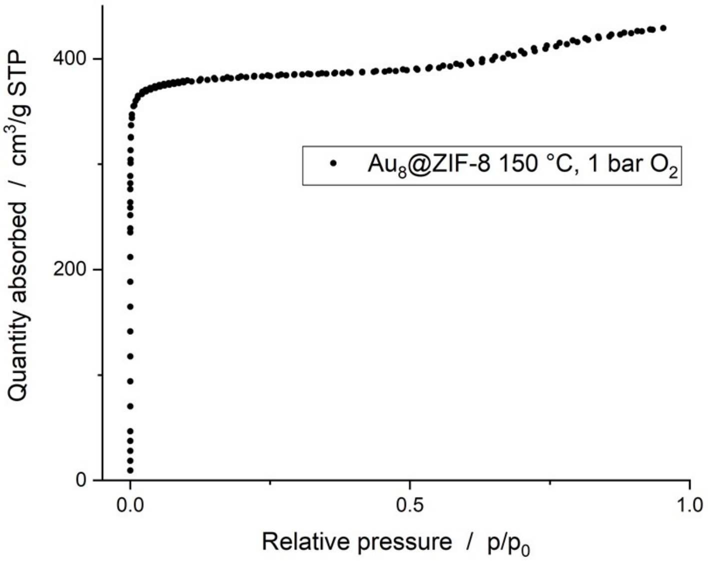

Figure S12: BET isotherm of **Au$_8$@ZIF-8** after treating at 150 °C under 1 bar$_g$ oxygen.

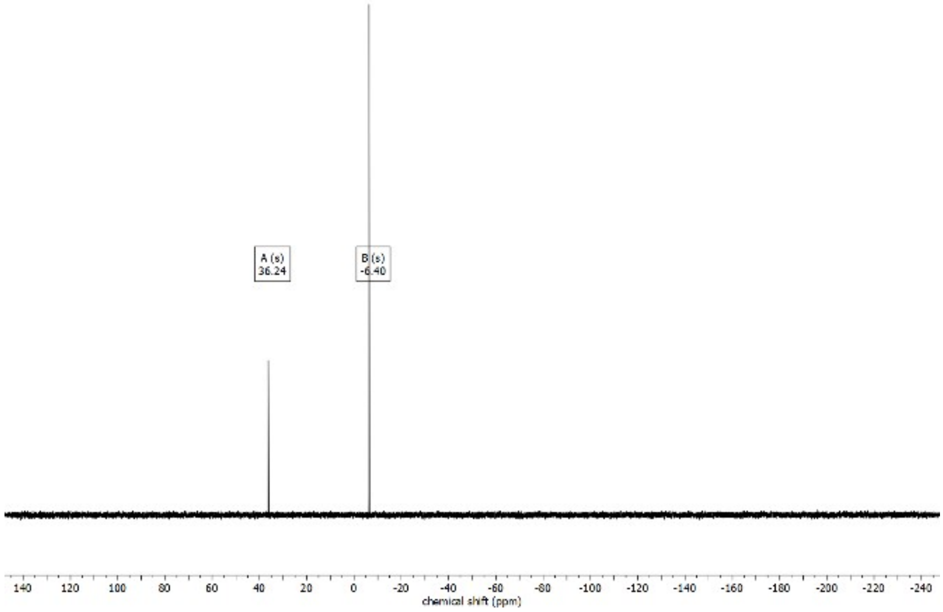

Figure S13: ^{31}P-NMR spectrum in D_2O of oxidised and pure TPPMS (observed at 36.24 and −6.40 ppm, respectively).

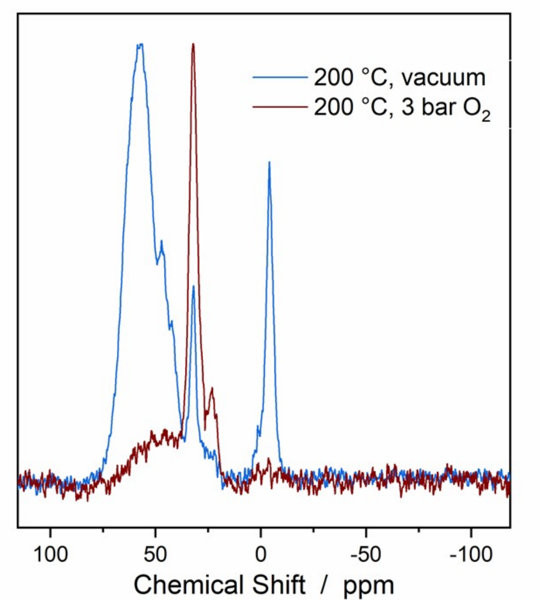

Figure S14: ^{31}P-MAS-NMR spectra of **Au_8@ZIF-8** after 200 °C vacuum and 3 bar$_g$ O_2 treatment, respectively, with one broad singlet peak at 57.4 ppm and two sharp singlet peaks at 32.0 and −4.1 ppm.

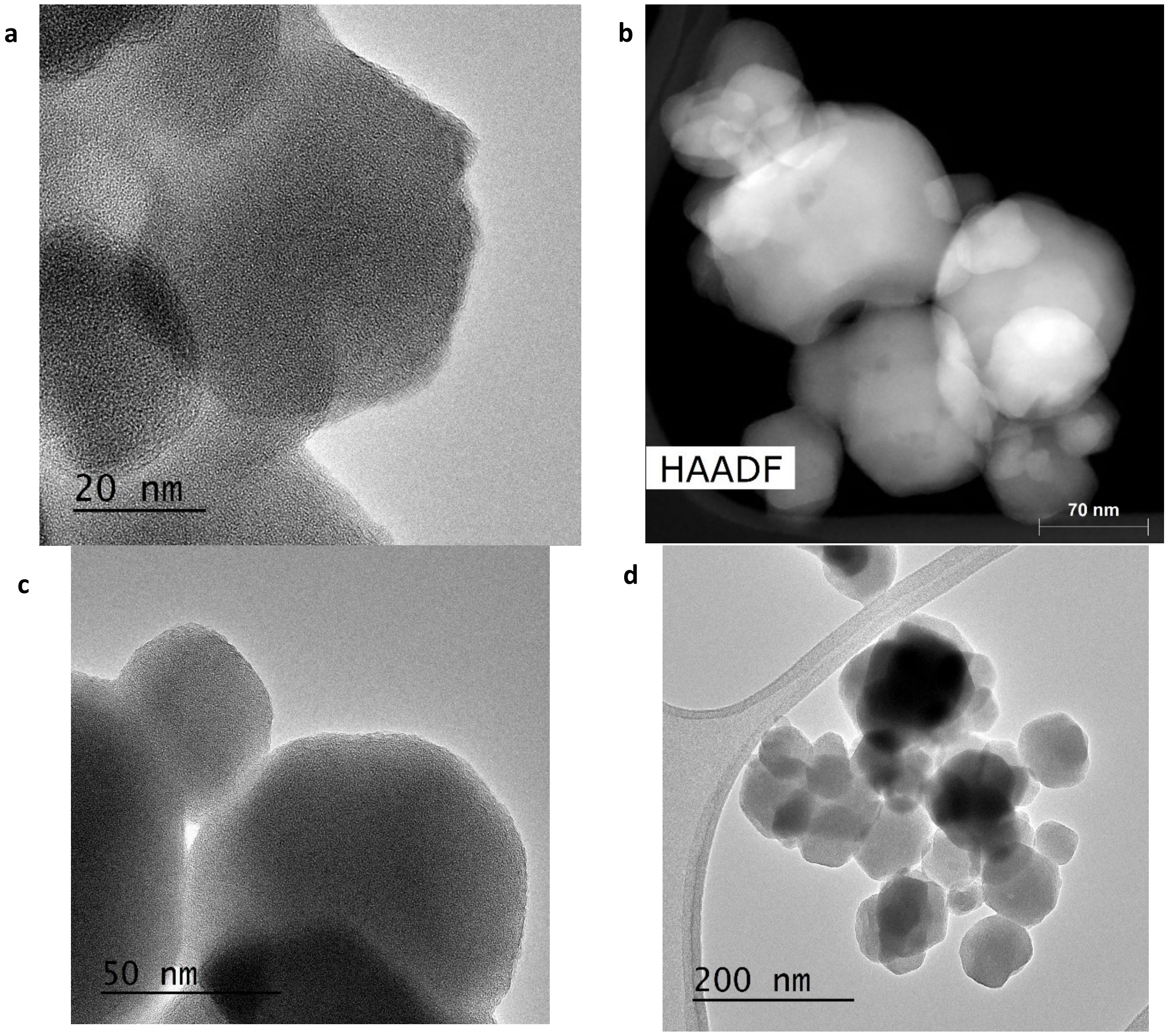

Figure S15: HR TEM and HAADF STEM of **Au$_8$@ZIF-8** after oxidative treatment at 150 °C, 1 bar$_g$ O$_2$

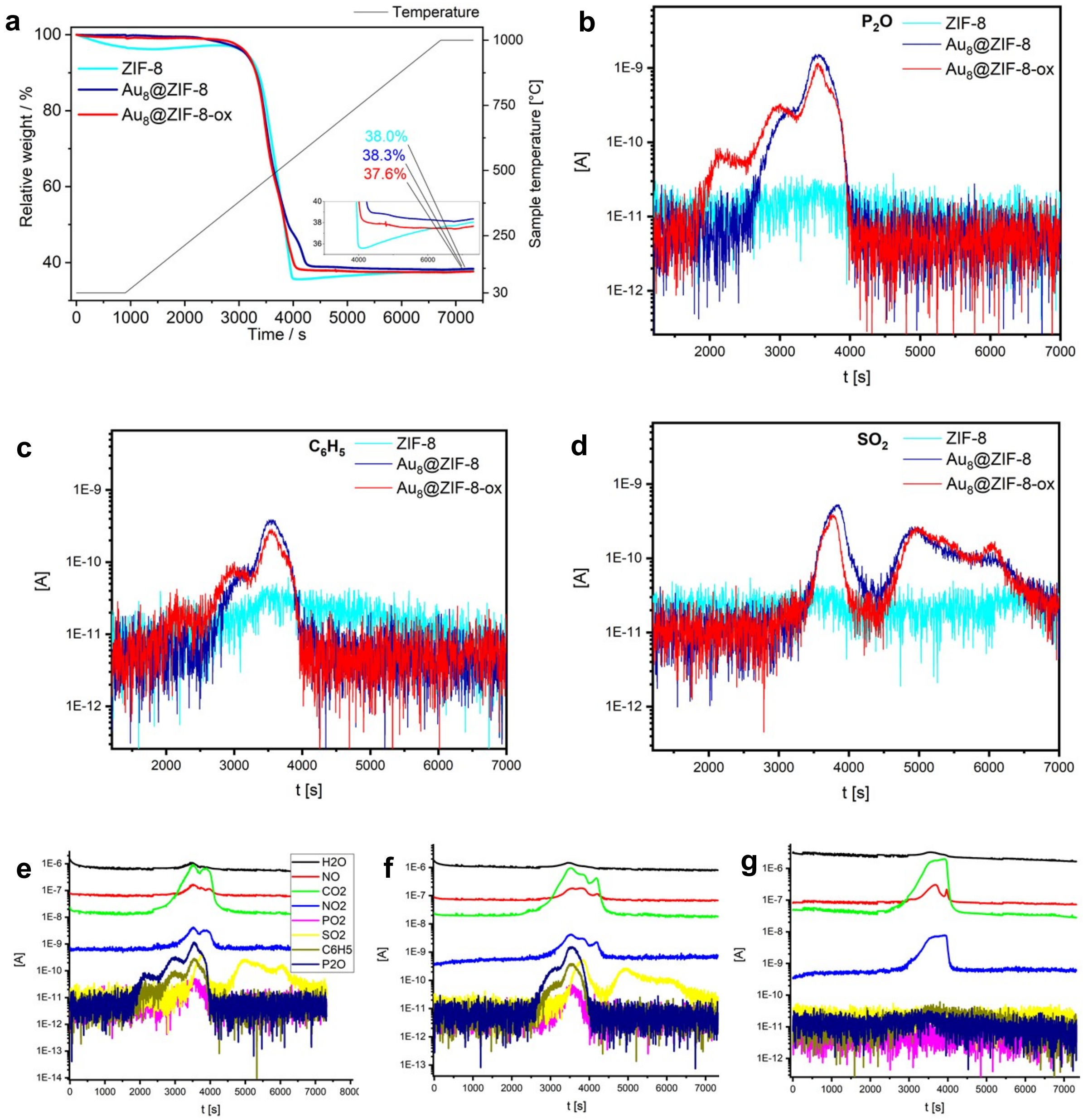

Figure S16: **a**, TGA curves of pristine ZIF-8, **Au$_8$@ZIF-8** and the oxidised material **Au$_8$@ZIF-8-ox** (200 °C, 3 bar$_g$ O$_2$); **b**, **c** and **d**, overlayed MS analysis of **Au$_8$@ZIF-8-ox**, **Au$_8$@ZIF-8** and pristine ZIF-8 for P$_2$O, C$_6$H$_5$, and SO$_2$, respectively; **e**, **f** and **g**, full MS analysis of **Au$_8$@ZIF-8-ox**, **Au$_8$@ZIF-8**, and pristine ZIF-8, respectively.

4. References

1 J. Rouquerol, P. Llewellyn and F. Rouquerol, in *Characterization of Porous Solids VII - Proceedings of the 7th International Symposium on the Characterization of Porous Solids (COPS-VII), Aix-en-Provence, France, 26-28 May 2005*, Elsevier, 2007, pp. 49–56.

2 M. Thommes, K. Kaneko, A. V. Neimark, J. P. Olivier, F. Rodriguez-Reinoso, J. Rouquerol and K. S.W. Sing, *Pure Appl. Chem.*, 2015, **87**, 1051–1069.

3 S. Liu, F. Chen, S. Li, X. Peng and Y. Xiong, *Appl. Catal. B: Environ*, 2017, **211**, 1–10.

4 R. L. Papporello, E. E. Miró and J. M. Zamaro, *Microporous Mesoporous Mat.*, 2015, **211**, 64–72.

5 Y. Pan, S. Neuss, A. Leifert, M. Fischler, F. Wen, U. Simon, G. Schmid, W. Brandau and W. Jahnen-Dechent, *Small*, 2007, **3**, 1941–1949.

6 G. Geng, P. Chen, B. Guan, Y. Liu, C. Yang, N. Wang and M. Liu, *RSC Adv.*, 2017, **7**, 51838–51846.